Abnormally Expressed Low-Voltage–Activated Calcium Channels in β-Cells From NOD Mice and a Related Clonal Cell Line

Lin Wang, Arin Bhattacharjee, Jian Fu, and Ming Li

A macroscopic low-voltage–activated (LVA) inward current was found in pancreatic β-cells isolated from NOD mice. However, this current was not present in nondiabetic prone mouse (e.g., Swiss-Webster) pancreatic β-cells. We performed pharmacological analyses on this current in NOD insulinoma tumor cells (NIT-1). This cell line was developed from pancreatic β-cells of a transgenic NOD mouse. The sodium-channel blocker, tetrodotoxin (TTX; 2 μmol/l) had no effect on this LVA current. The amplitudes of currents elicited by a –20 mV test pulse retained similarity when the extracellular sodium concentration was increased from 0 to 115 mmol/l; when the extracellular calcium concentration was decreased from 10 to 2 mmol/l, there was an approximate 50% reduction of this current elicited by a –30 mV test pulse. Neither the L-type calcium-channel blocker, nifedipine (3 μmol/l), nor the N-type calcium-channel blocker, ω-CgTx-GVIA (1 μmol/l), at –30 mV produced an appreciable effect. The T-type calcium-channel blockers, nickel (3 μmol/l) and amiloride (250 μmol/l), effectively reduced the peak of this current. In 2 mmol/l calcium external solution, the threshold of voltage-dependent activation of this calcium current was approximately –65 mV, and the peak current occurred at –20 mV. Half-maximum steady-state inactivation was around –43 mV. The mean time constant of slow deactivating tail currents generated by a preceding 20 mV pulse was 2.53 ms. The intracellular free calcium concentration was two- to threefold higher in NOD mouse pancreatic β-cells compared with Swiss-Webster pancreatic β-cells. We concluded that there are LVA calcium channels abnormally expressed in NOD mouse β-cells. This LVA calcium channel may be factorial to the high cytosolic free calcium concentration observed in these cells, and thereby may contribute to the pathogenesis of NOD mouse β-cells. *Diabetes* 45:1678–1683, 1996

From the Department of Pharmacology, University of South Alabama, College of Medicine, Mobile, Alabama.

Address correspondence and reprint requests to Ming Li, PhD, Department of Pharmacology, University of South Alabama, College of Medicine, Mobile, AL 36688. E-mail: mli@jaguar1.usouthal.edu.

Received for publication 29 January 1996 and accepted in revised form 26 July 1996.

BAPTA, bis(2-aminophenoxy)ethane-*N*,*N*,*N*′,*N*′-tetraacetate; FBS, fetal bovine serum; HEPES, 10 N-2-hydroxyethylpiperazine-*N*′-2-ethanesulfonic acid; HVA, high voltage–activated; LVA, low-voltage–activated; NIT, NOD insulinoma tumor; P/S, penicillin 25 U/ml and streptomycin 25 μg/ml; TEA-Cl, tetraethylammonium-Cl; TEA-OH, tetraethylammonium-OH; TTX, tetrodotoxin.

IDDM is an autoimmune disease associated with the destruction of the insulin-producing pancreatic β-cells (1). Environmental factors such as microbial agents and chemicals act as triggers of an autoimmune response against pancreatic islet β-cells in a genetically diabetes-prone phenotype (2). However, the mechanisms of cell death are not completely understood.

Increases in intracellular free calcium concentration have been linked to cell death in a number of experimental systems. Internucleosomal DNA cleavage by Ca^{2+}- and Mg^{2+}-dependent endonucleases, activated by intracellular calcium uptake, is a characteristic marker of programmed cell death. Serum from IDDM patients has been shown to increase voltage-dependent calcium channel activity in insulin-producing cells. The subsequent increase in the concentration of free cytoplasmic calcium has been associated with DNA fragmentation and β-cell destruction (3).

We decided to explore further the calcium channel profile of diabetes-prone β-cells, specifically from the NOD mouse (4) and a β-cell line generated in insulinoma tumor cells from transgenic NOD mice (NIT-1) (5). NOD mice develop a spontaneous type of diabetes that resembles human IDDM, including abrupt onset between 90 and 120 days (equivalent to early adolescence in humans), hyperglycemia, glycosuria, and polyphagia. Furthermore, it has been demonstrated that cytokine-induced DNA fragmentation precedes cell lysis in rat insulinoma cells (RINm5F) and NIT-1 cells, but not in non–islet cell lines (6). In this study, we demonstrated the presence of abnormally expressed LVA calcium channels in NOD mouse pancreatic β-cells and NIT-1 cells. We found increased levels of free cytoplasmic calcium concentrations in NOD mouse pancreatic β-cells that might result from this LVA calcium current.

RESEARCH DESIGN AND METHODS

Islet cell preparation. The pancreases of NOD mice (The Jackson Laboratory, Bar Harbor, ME; 8–10 weeks old) and Swiss-Webster mice (Charles River Laboratory, Wilmington, MA; 8–10 weeks old) were removed after intrapancreatic perfusion with 2 ml of Hanks' solution (Gibco BRL, Grand Island, NY) containing collagenase (4 mg/ml, Boehringer Mannheim, Indianapolis, IN), DNase I (10 μg/ml; Sigma, St. Louis, MO), $CaCl_2$ (1.28 mmol/l), and bovine serum albumin (1 mg/ml). The pancreatic tissue was then incubated at 37°C for 20 min and washed five times with enzyme-free Hanks' solution. The islets were picked up and transferred into a 1.5-ml centrifuge tube. Single cells were obtained by triturating the islets using plastic pipette tips and then transferring them into 35-mm culture dishes. Cells were then cultured in RPMI 1640 medium (Gibco BRL) containing 5 mmol/l glucose,

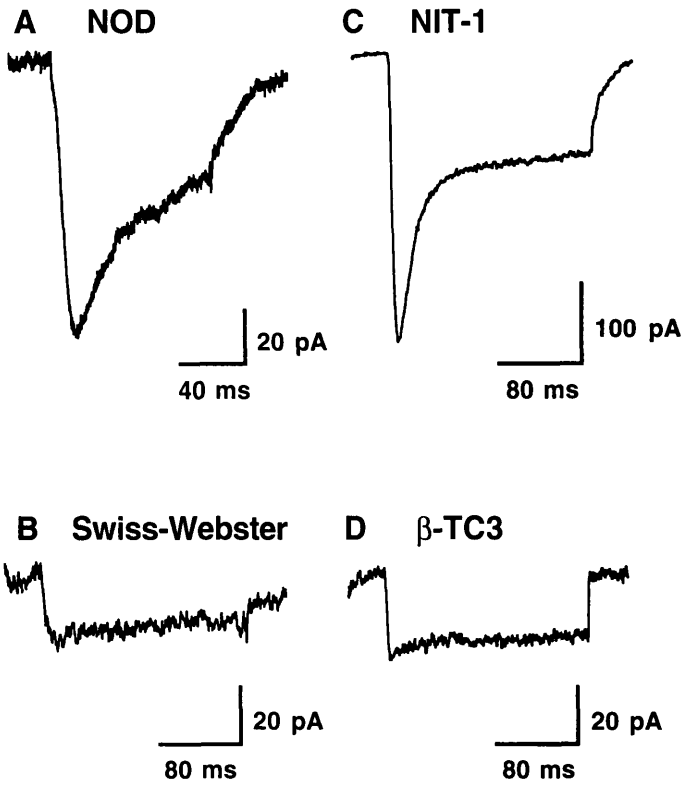

FIG. 1. Barium currents were recorded in a primary cultured pancreatic β-cell of NOD mouse (*A*), a primary cultured pancreatic β-cell of Swiss-Webster mouse (*B*), an NIT-1 cell (*C*), and a β-TC3 cell (*D*). The recordings were all elicited by a voltage step from –70 to –10 mV.

10% fetal bovine serum (FBS), and P/S (penicillin 25 U/ml; streptomycin 25 μg/ml) at 37°C, 5% CO_2, for 2–5 days before recording.

Cell culture. NIT-1 cells and β-TC3 (a β-cell line derived from nondiabetic transgenic mice) cells (7) were cultured in RPMI 1640 medium containing 5 mmol/l glucose, 10% FBS, and P/S in an atmosphere of 5% CO_2 in air at 37°C. The cells were patch clamped 2–5 days after plating. NIT-1 and β-TC3 cells were kindly provided by Dr. Richard E. Honkanen (University of South Alabama) and Dr. Joel F. Habener (Harvard Medical School), respectively.

Patch clamp electrophysiology and data analysis. The whole-cell recordings were carried out by the standard "giga-seal" patch clamp technique (8). The whole-cell recording pipettes were made of hemocapillaries (Fisher Scientific, Pittsburgh, PA), pulled by a two-stage puller (P-30, Sutter Instrument, Novato, CA), and heat polished before use. Pipette resistance was in the range of 2–3 MΩ in our internal solutions. The access resistance was typically 10 MΩ, which predicts a 1-mV voltage error for the peak current of 100 pA. The recordings were performed at room temperature (22–25°C). Currents were recorded using an EPC-9 patch-clamp amplifier (HEKA, Lambrecht/Pfalz, Germany) and filtered at 2.9 kHz. Data were acquired with Pulse/PulseFit software (HEKA). Voltage-dependent currents were corrected for linear leak and residual capacitance by using an on-line P/n subtraction paradigm. Normalized conductance-voltage relationship curves and steady-state inactivation curves were fitted with the Boltzmann equation, $1/[1 + \exp[(V - V_{1/2})/k]]$, where $V_{1/2}$ is the voltage of half activation and k is a slope factor. (Pooled data are reported as means ± SE in the text and in figure legends.)

Solutions for recording. The high calcium extracellular solution contained (in mmol/l): 10 $CaCl_2$, 110 tetraethylammonium-Cl (TEA-Cl), 10 CsCl, 10 *N*-2-hydroxyethylpiperazine-*N'*-2-ethanesulfonic acid (HEPES), 40 sucrose, 0.5 3,4-diaminopyridine, pH 7.3. The low calcium extracellular solution contained (in mmol/l): 2 $CaCl_2$, 110 TEA-Cl, 10 CsCl, 10 HEPES, 40 sucrose, 0.5 3,4-diaminopyridine, pH 7.3. The barium extracellular solution contained (in mmol/l): 40 $Ba(OH)_2$, 30 tetraethylammonium-OH (TEA-OH), 5 TEA-Cl, 10 HEPES, 100 sucrose, pH 7.3. The standard intracellular solution contained (in mmol/l): 130 *N*-methyl-D-glucamine, 20 EGTA (free acid), 5 bis(2-aminophenoxy)ethane-*N,N,N',N'*-tetraacetate (BAPTA), 10 HEPES, 6 $MgCl_2$, 4 $Ca(OH)_2$, with pH adjusted to 7.4 with methanesulfonate. The free calcium concentration of the intracellular solution was estimated to be 2.3×10^{-8} mol/l using association constants previously reported (9). In some experiments, 2 mmol/l Mg ATP and 1 mmol/l ATPγS were included in the pipette solution to minimize rundown of Ca^{2+} currents.

Intracellular free calcium measurements. For fluorescence measurements, the cells were cultured on Poly-D-Lysine (50 μg/ml, Sigma) –coated glass coverslips (No. 1 grade, Fisher) for 2–4 days. The cells were then loaded with the Ca^{2+}-sensitive dye Indo-1 by incubation for 20 min at 37°C in an extracellular solution (150 mmol/l NaCl, 4 mmol/l KCl, 5 mmol/l glucose, 2 mmol/l $CaCl_2$, 2 mmol/l $MgCl_2$, and 5 mmol/l HEPES; pH 7.2) containing 2.5 μmol/l Indo-1 AM (Molecular Probes, Eugene, OR). After being washed, the chamber was then mounted in the ACAS 570 interactive confocal laser cytometer (Meridian Instruments, Okemos, MI). Dual monitors provided simultaneous fluorescence and video-image displays. This allowed us to compare the light optical and fluorescence images. The cells were illuminated by the 351-nm to 363-nm lines of the tunable 5-W argon ion ultraviolet-visible laser, and the Indo-1 fluorescence was recorded (× 100 oil objective) at 405 (Ca^{2+}-bound) and 485 (Ca^{2+}-free) nm wavelengths (10). The intracellular free calcium concentration was measured in the image scan mode. The laser scan strength was set at 10–30% of the 50-mW output, and a 1% neutral density filter was used. The ratio of emissions at two fluorescent wavelengths was converted to the free calcium concentration by a standard curve. The standard curve was generated using known incremental concentrations of calcium. Specifically, 1 μl Orion calcium standard (100 mmol/l stock, Molecular Probes) was added into 1 ml Indo-1 buffer (10 μmol/l indo free acid, 100 mmol/l KCl, 1 mmol/l EGTA, 50 mmol/l HEPES; pH 7.2, K_D = 0.151 μmol/l) to increase total calcium by 100 μmol/l each time. Approximately 10 such additions were made for a total added calcium concentration of about 1,000 μmol/l. Scans were completed after each addition.

RESULTS

We found an LVA calcium current in NOD mouse β-cells but not in Swiss-Webster mouse β-cells.

Figure 1*A* shows a fast inactivating inward current (barium as carrier) recorded at –10 mV test potential when the membrane was held at –70 mV in a pancreatic β-cell from NOD mouse. This fast inactivating inward current was observed in 7 of 10 cells where measurable inward barium currents were detected. The inactivation time constants of this inward current at –20 mV were approximately 20–30 ms. In contrast, no such current was observed in the primary cultured β-cells of Swiss-Webster mice (n = 14). We found only high voltage–activated (HVA) barium currents with an activation threshold of approximately –20 mV, peaking at 20 mV. This HVA barium current did not inactivate for 200 ms at the test potential of –10 mV (Fig. 1*B*). The absence of LVA calcium current (a fast inactivating inward current) in Swiss-Webster mouse β-cells is consistent with previous findings from other researchers (11–14).

Mouse pancreatic islets consist mainly of β-cells, yet they also contain other cell types. To ensure that this fast inactivating inward current is present in mouse β-cells, we studied barium currents in NIT-1 cells. Figure 1*C* shows a fast inactivating inward current recorded at –10 mV in an NIT-1 cell; this current was observed in almost all of the cells recorded. In contrast, the barium currents (Fig. 1*D*) recorded at –10 mV in β-TC3 cells retained only the HVA calcium current, similar to the results observed in Swiss-Webster mouse β-cells.

To further substantiate that this fast inactivating inward current is a calcium-selective current rather than an abnormal sodium current, we administered 2 μmol/l tetrodotoxin (TTX) into the extracellular solution. Figure 2*A* shows that TTX had no effect on this inward current. Figure 2*B* shows that the amplitudes of the currents remained similar in the extracellular solutions containing

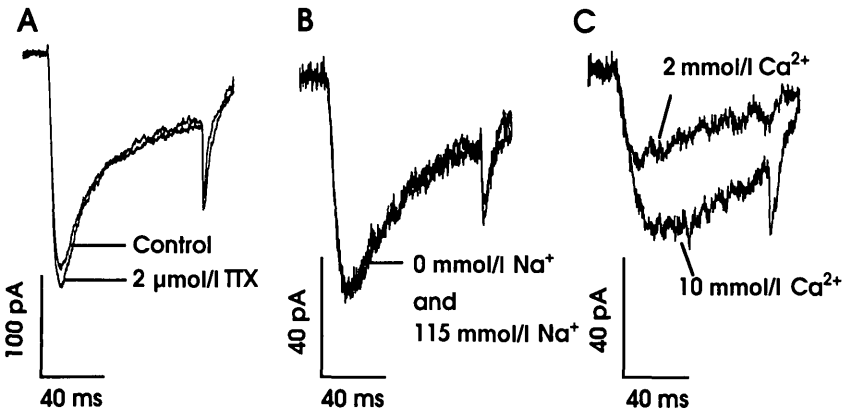

FIG. 2. Effects of TTX (*A*), change of extracellular Na^+ concentration (*B*), and change of extracellular Ca^{2+} concentration (*C*) on the fast inactivating currents in NIT-1 cells. Experiments were performed in 10 mmol/l calcium external solution and currents were measured at –20 mV in *A* and *B*. In *B*, the cell was bathed in an extracellular solution containing 110 mmol/l TEA-Cl and 40 mmol/l sucrose; the bath solution was then replaced by 20 mmol/l TEA-Cl and 115 mmol/l NaCl. In *C*, the initial bath solution contained 10 mmol/l calcium; it was then replaced by a 2 mmol/l calcium solution. The test potential in *C* was at –30 mV. All experiments were held at –70 mV.

either 0 or 115 mmol/l sodium. These results suggest that the fast inactivating inward current is not mediated by either sodium channels or nonselective cation channels. However, changing the extracellular calcium concentration from 10 mmol/l to 2 mmol/l resulted in an approximate 50% reduction of this inward current elicited by a –30 mV test pulse (Fig. 2*C*). This result suggests that the inward current is a calcium-selective current.

Pharmacological analyses were performed to identify this fast inactivating calcium current in NIT-1 cells. To determine if this current was an L-type calcium current, we tested the effect of nifedipine, a drug that preferentially targets L-type calcium channels. Figure 3*A* shows that the amplitude of this inward current was reduced only slightly by 3 μmol/l nifedipine. Similar results were obtained from 33 other experiments. This inward current was also insensitive to ω-conotoxin, an N-type calcium channel selective antagonist (Fig. 3*B*). Administration of 1 μmol/l ω-CgTx-GVIA only slightly reduced this current (n = 4). These results demonstrated that this abnormally expressed fast inactivating calcium current found in NIT-1 cells is insensitive to nifedipine and ω-conotoxin.

Although the LVA calcium current has not been observed in mouse β-cells, we were interested in testing the hypothesis that this fast inactivating calcium current is indeed an LVA current expressed in NIT-1 cells. Figure 3*C* shows a family of barium current traces recorded at variable test potentials with a holding potential of –70 mV. The current first appeared at –40 mV and exhibited both a fast inactivating and a sustained component. However, in the same experiment, when the holding potential was changed to –40 mV, the fast inactivating component was no longer observed. Only sustained currents were observed (Fig. 3*D*), which first appeared at –20 mV and peaked at 10 mV. Thus the fast inactivating calcium current observed in NOD mouse β-cells and NIT-1 cells is reminiscent of the LVA calcium current seen in human and rat pancreatic β-cells, but not in other mouse pancreatic β-cells (15–18).

It has been shown that nickel selectively blocks T-type calcium channels (19–21). Figure 4*A* shows that perfusion of the recording chamber with a solution containing 2 μmol/l $NiCl_2$ blocked 50% of the calcium current elicited by depolarizing to –30 mV, a potential at which HVA calcium current was not activated in our experimental conditions. The effect of nickel on LVA calcium current was reversible after washout. Figure 4*B* shows the dose-response curve of the effect of nickel. The half-maximal inhibition was approximately 3 μmol/l nickel, whereas 90% blockade required a high nickel concentration of 200 μmol/l.

It has been also shown that amiloride, a diuretic agent, effectively blocks T-type calcium channels in neurons and heart muscle cells, but has little effect on L-type currents (22–24). Figure 4*C* shows the inhibitory effect of 200 μmol/l amiloride on the LVA current recorded in an NIT-1 cell. This effect of amiloride was also reversible on wash-out. Figure 4*D* shows the dose-response curve of amiloride blockade of the LVA current in NIT-1 cells; the half-maximum inhibition required ~280 μmol/l amiloride. Thus the pharmacological analyses suggest that the LVA current in NIT-1 cells is a T-type calcium current.

The current-voltage relationships of the LVA calcium currents in NOD mouse β-cells and NIT-1 cells are shown in Fig. 5*A* and Fig. 5*B*, respectively. With 40 mmol/l barium in the extracellular solution, inward calcium currents have a threshold near –50 mV, and develop rapidly as a function of voltage; the peak current is close to –20 mV. Because the L-type calcium current did not inactivate during a 200-ms test pulse, the sustained currents in NIT-1 cells were also measured as a function of voltage (plotted as filled circles in Fig. 5*B*). This current consists mainly of the L-type current component, which has a threshold near –20 mV and peaks at 20 mV, similar to the result shown in Fig. 3*D*.

In rat pancreatic β-cells, LVA calcium currents are distinguished from L-type currents by their slow deactivation (15). In Fig. 5*C*, tail currents were recorded at –90 mV with 10-ms prepulses varying from –60 mV to 20 mV. Figure 5*D* shows the average τ of the slow component of the tail currents, which was 2.53 ± 0.293 ms (n = 10) in response to a prepulse of 20 mV. This value is similar to that of LVA currents reported in rat β-cells (2.8 ms). In contrast, the averaged τ of the fast component (generated from L-type currents) of the tail currents was 223 ± 44.8 μs (n = 3; L-type current in some cells were too small to be measured) after prepulses ranging to 40 mV.

In 2 mmol/l Ca^{2+} external solution, analysis of activation and inactivation of the LVA calcium current revealed a "window" of voltages, where activation and inactivation curves overlap (Fig. 5*E*). At these voltages, the LVA calcium channels show some degree of activation, but are not yet completely inactivated, as a theoretical "window" current will flow into cells. The magnitude of this steady-state current can be determined as a function of voltage

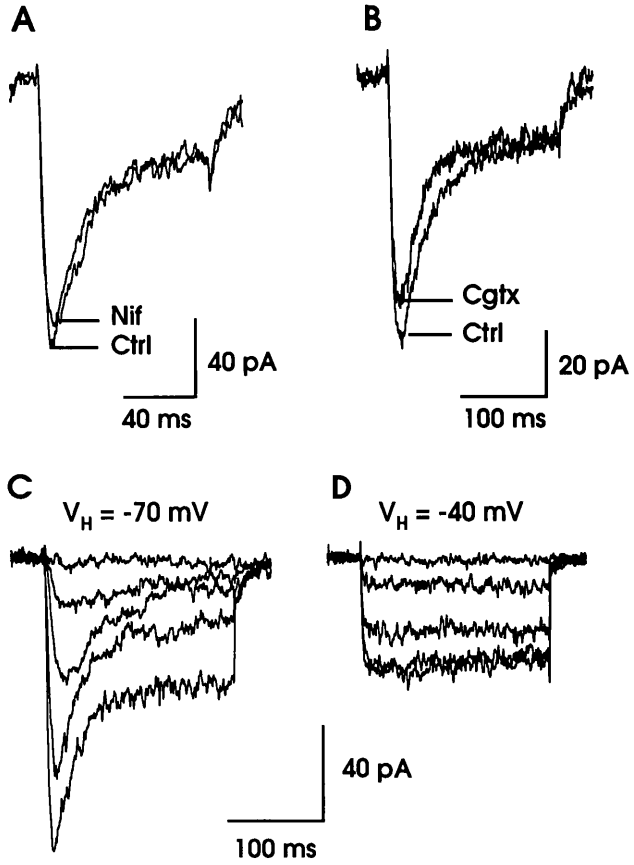

FIG. 3. The effects of nifedipine (*A*) and ω-conotoxin (*B*) on the fast inactivating currents. Experiments were performed in 40 mmol/l barium external solutions. The currents were recorded at –30 mV and stepped from –70 mV. *C*: a family of barium current traces were measured at –50, –40, –30, –20, and –10 mV, with a holding potential of –70 mV. *D*: in the same experiment as *C*, family traces of barium currents were measured at –30, –20, –10, 0, and 10 mV, with a holding potential of –40 mV. Ctrl, control; Nif, 3 μmol/l nifedipine; Cgtx, 1 μmol/l ν-CgTx-GVIA.

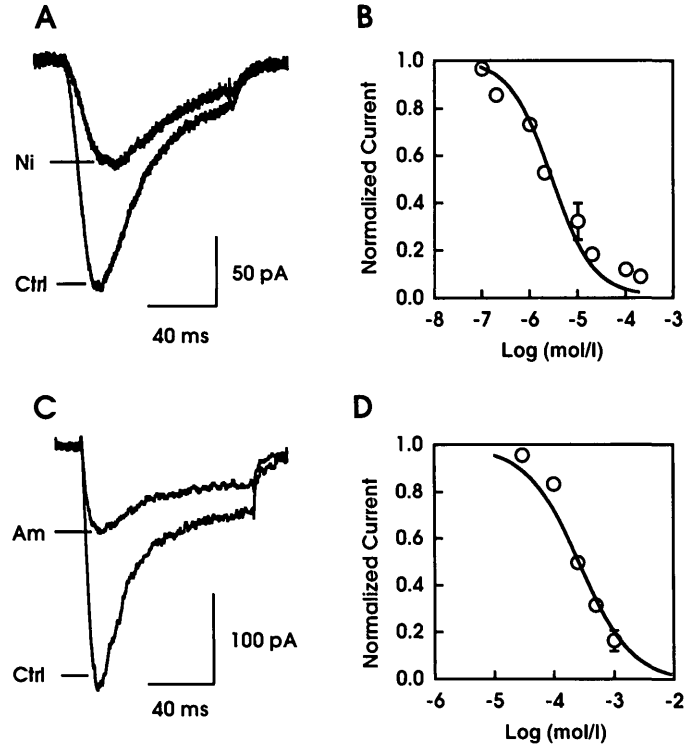

FIG. 4. Effects of nickel and amiloride on LVA calcium currents in NIT-1 cells. *A*: the LVA currents were elicited by –30 mV test pulses and held at –70 mV. *B*: concentration dependent blockade of the LVA currents by $NiCl_2$, n = 4. *C*: the LVA currents were recorded at –30 mV and held at –80 mV. *D*: concentration-dependent blockade of the LVA currents by amiloride, n = 3. In *B* and *D*, all currents were normalized, with the current amplitude measured before $NiCl_2$ or amiloride perfusion. Error bars indicate SE. Smooth lines are plots of theoretical Michaelis-Menten-type curves with Kd of 3 μmol/l and 287 μmol/l for $NiCl_2$ and amiloride, respectively. All experiments were performed in 10 mmol/l calcium external solution. Ni, $NiCl_2$; Am, amiloride; Ctrl, control.

using Ohm's Law (25) (Fig. 5*F*). At voltages between –60 and –50 mV, there will be a maximum steady-state calcium entry through these LVA channels. At the more positive potentials, it will decay within a few seconds.

The high-level expression of LVA calcium channels in NOD mouse pancreatic β-cells may enhance the basal calcium influx, thus elevating cytoplasmic free calcium concentration. To test this hypothesis, we used Indo-1 AM to measure the basal intracellular free calcium concentration in primary cultured β-cells isolated from Swiss-Webster mice and NOD mice. Figure 6 shows that basal intracellular free calcium concentration is two- to threefold higher in NOD mouse β-cells (n = 11) than in Swiss-Webster cells (n = 7). All experiments were conducted in medium containing 5 mmol/l glucose. This result indicates that the intracellular free calcium concentration of NOD mouse β-cells is abnormally high under nonstimulatory conditions.

DISCUSSION

Studies in kinetics, selectivity, and pharmacology have indicated an abnormally expressed LVA calcium current in NOD mouse β-cells and NIT-1 cells. This current may facilitate spontaneous elevation of intracellular free Ca^{2+}, as described in *Xenopus* neurons (26). The sizable LVA "window" current may directly lead to increased intracellular calcium levels.

The presence of LVA currents may also prematurely trigger the L-type calcium channel–dependent action potentials, as well as enhance calcium influx in response to glucose elevation in mouse β-cells. Although insulin release response to 5 mmol/l glucose was not altered in NIT-1 cells (5), enhanced excitability may occur at higher glucose concentrations because of the LVA current.

Enhanced excitability and cytoplasmic Ca^{2+} overload resulting from overexpression of LVA calcium currents have been suggested to play crucial roles in the pathogenesis of several model systems of human diseases, including cardiomyopathic hamster heart (27), hypertrophied adult feline left ventricular myocytes (28), rat neointima formation after vascular injury (29), and the generation of spike-wave discharges in petit mal epilepsy in guinea pig thalamic neurons (30). LVA calcium channels have also been shown to mediate sustained increases in intracellular calcium induced by angiotensin II (31), endothelin (32), and platelet-derived growth factor (33). A sustained increase in intracellular calcium is capable of activating a number of potentially harmful

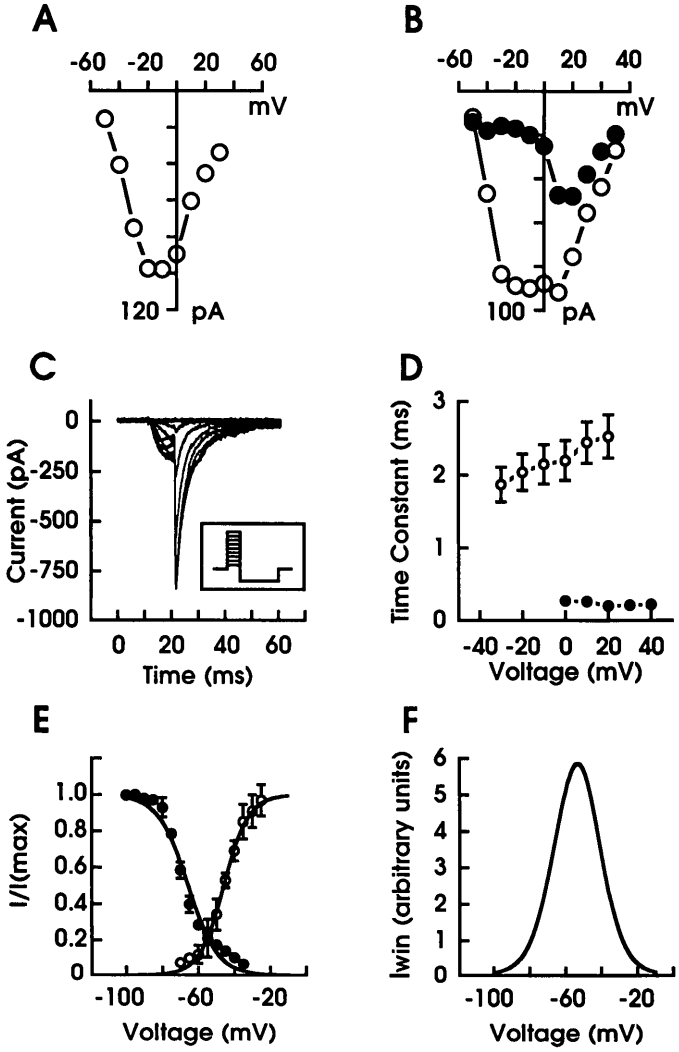

FIG. 5. Current-voltage relationships of barium currents obtained from a primary cultured NOD mouse β-cell (*A*) and from a NIT-1 cell (*B*). The open circles in *B* represent the peak currents measured at the first 50 ms duration of the 200-ms depolarizing pulses and the filled circles represent the currents measured at the last 50 ms duration of the pulses. The holding potential was at –80 mV. *C*: tail currents recorded from NIT-1 cells; voltage protocol shown inside. Currents were measured at –90 mV with 10-ms prepulses stepped from –70 mV to voltages varying from –60 to 20 mV. *D*: plot of slow (○, n = 10) and fast (●, n = 3) deactivating time constants as a function of the prepulse voltages. *C* and *D* were performed in an extracellular solution containing 10 mmol/l Ca^{2+}. *E*: activation and inactivation curves of LVA channels in NIT-1 cells using 2 mmol/l Ca^{2+} external solution. The channel conductances (represented by normalized tail currents) were plotted as a function of prepulse voltage (activation). The inactivation data was generated with a protocol consisting of 3-s prepulses ranging from –100 to –35 mV followed immediately by test pulses (200 ms) to –30 mV. Both activation and inactivation data were normalized to the maximum of the functions and fitted to the Boltzmann equation ($V_{1/2}$ = –45.2 mV, k = –6.93, n = 4 for activation curve; $V_{1/2}$ = –65.64 mV, k = 8.28, n = 4 for inactivation curve). *F*: the theoretical peak "window" current is determined as a function of voltage from the Ohm's equation: $I_w = g_{Ca}mh\ (V_{rev} - V)$, where g_{Ca} is the maximal calcium conductance through T-type calcium channels (when all channels are open) and arbitrarily chosen equal to 1.0, m and h are the fractions of open channels (I/I_{max}), calculated from the Boltzmann equation in activation and inactivation experiments, respectively, and V_{rev} is the reversal potential extrapolated to be 70 mV. For *E* and *F*, the recordings were performed on the cells that had minimal HVA currents.

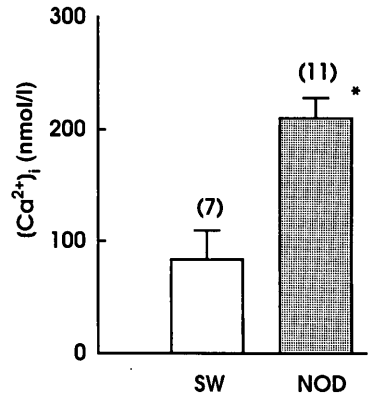

FIG. 6. Intracellular free calcium concentrations measured from Swiss-Webster mouse β-cells and NOD mouse β-cells. Cells were loaded with 2.5 μmol/l Indo-1 AM and bathed in a solution containing 5 mmol/l glucose. *P < 0.01, significance in calcium concentration as determined using Student's t test. SW, Swiss-Webster mice; NOD, nonobese diabetic mice.

processes in the cell. Some of these mechanisms involve the activation of hydrolytic enzymes such as phospholipase A_2, Ca^{2+}-activated proteases, and Ca^{2+}-activated endonucleases, whereas others include modulation of signaling pathways, including ligand-activated kinases as well as intracellular messengers (34). Abnormally expressed LVA calcium current in NOD mouse β-cells may directly or indirectly participate in the process of β-cell destruction through one or more of these mechanisms. For example, it has been demonstrated that DNA fragmentation is an early event in cytokine-induced NIT-1 and RINm5F cell destruction (6). Similar results have been reported in IDDM patient serum–mediated RINm5F cell destruction (3). In the latter case, the roles of free cytosolic calcium and voltage-dependent calcium channels in DNA fragmentation were clearly demonstrated. Abnormally expressed LVA current in NOD mouse pancreatic β-cells may result in altered Ca^{2+} homeostasis, produced by enhanced calcium influx at lower membrane potentials and mediated by a higher excitability response to insulin secretagogues. These may contribute to the pathogenesis of β-cells.

LVA calcium currents have been reported in human and rat pancreatic β-cells, where they are a minor component of total calcium influx; however, their physiological function for insulin secretion is not completely understood. The LVA calcium currents in NOD mouse β-cells and NIT-1 cells exhibit similar properties to LVA calcium currents in human and rat β-cells. The high expression of LVA calcium current in NIT-1 cells provides a model system to elucidate the possible physiological role of calcium currents in membrane excitability and cytoplasmic free calcium regulation in human β-cells.

L-type calcium currents have been suggested to be responsible for resting intracellular Ca^{2+} concentration and basal insulin release in mouse β-cells (35). Our results suggest that overexpression of LVA calcium channels may be additive, and may play a more important role in these functions in NOD mouse and NIT-1 cells, since a theoretical "window" current may be present at low membrane potentials (–60 to –50 mV) in these cells (Fig. 5*F*).

It has been reported that a 10-s depolarizing command pulse elicits the fast and slow inactivating calcium currents in Swiss-Webster mouse pancreatic β-cells (36); the observed fast inactivating current meets some of the criteria of T-type calcium current. In our experimental conditions, however, this corresponding fast inactivation component was not detected in the primary cultured β-cells of Swiss-Webster mice.

The high expression of LVA calcium current was not accompanied by a decrease of L-type calcium current in NIT-1 cells (Figs. 3*C* and 5*B*). The sensitivities to nickel, amiloride, and nifedipine are different for LVA currents and L-type currents. These results argue that the LVA calcium channel may not be a modified form of the L-type calcium channel in β-cells, but may be a distinct protein.

Other calcium transport systems in mouse β-cells, such as Na^+/Ca^{2+} exchange, Ca^{2+}-ATPase, and various intracellular calcium stores, also play important roles in regulating the free cytoplasmic calcium level. It is not known if these systems function normally in NOD mouse pancreatic β-cells and NIT-1 cells. Nevertheless, the study of abnormal expression of LVA calcium current in the pancreatic β-cells of diabetes-prone NOD mice increases our understanding of the multitude of clinical complications observed in IDDM.

ACKNOWLEDGMENTS

This work was supported by Research Starter Grant and Faculty Development Award from the PhRMA Foundation, and a Career Development Award from the American Diabetes Association to M.L.

We thank Dr. S. Misler for many important suggestions to the work. We thank Dr. T. Scheuer, Dr. A. Sculptoreanu, and Dr. R.M. Whitehurst for critical reading of the manuscript and Dr. P.-O. Berggren for valuable discussions.

REFERENCES

1. Eisenbarth GS: Type I diabetes mellitus: a chronic autoimmune disease. *N Engl J Med* 314:1360–1368, 1985
2. Eisenbarth GS, Ziegler AG, Colman PA: Pathogenesis of non-insulin-dependent (type I) diabetes mellitus. In *Joslin's Diabetes Mellitus*. 13th ed. Kahn CR, Weir GC, Eds. Malvern, PA, Lea & Febiger, 1994, p. 216–239
3. Juntti-Berggren L, Larsson O, Rorsman P, Ämmälä C, Bokvist K, Wåhlander K, Nicotera P, Dypbukt J, Orrenius S, Hallberg A, Berggern P-O: Increased activity of L-type Ca^{2+} channels exposed to serum from patients with type I diabetes. *Science* 261:86–90, 1993
4. Makino S, Kunimoto K, Muraoka Y, Mizushima Y, Katagiri K, Tochino Y: Breeding of a non-obese, diabetic strain of mice. *Exp Anim* 29:1–3, 1980
5. Hamaguchi K, Gaskins HR, Leiter EH: NIT-1, a pancreatic β-cell line established from a transgenic NOD/Lt mouse. *Diabetes* 40:842–849, 1991
6. Rabinovitch A, Suarez-Pinzon WL, Shi Y, Morgan AR, Bleackley RC: DNA fragmentation is an early event in cytokine-induced islet beta-cell destruction. *Diabetologia* 37:733–738, 1994
7. Efrat S, Leiser M, Surana M, Tal M, Fusco-Demane D, Fleischer N: Murine insulinoma cell line with normal glucose-regulated insulin secretion. *Diabetes* 42:901–907, 1993
8. Hamill OP, Marty A, Neher E, Sakmann B, Sigworth FJ: Improved patch-clamp techniques for high-resolution current recording from cells and cell-free membrane patches. *Pflügers Arch* 391:85–100, 1981
9. Fabiato A, Fabiato F: Calculator programs for computing the composition of the solutions containing multiple metals and ligands used for experiments in skinned muscle cells. *J Physiol Paris* 75:463–505, 1979
10. Luckoff A: Measuring cytosolic free calcium concentration in endothelial cells with Indo-1: the pitfall of using the ratio of two fluorescence intensities recorded at different wavelengths. *Cell Calcium* 7:233–248, 1986
11. Rorsman P, Ashroft FM, Trube G: Single Ca channel currents in mouse pancreatic B-cells. *Pflügers Arch* 412:597–603, 1988
12. Smith PA, Rorsman P, Ashcroft FM: Modulation of dihydropyridine-sensitive Ca^{2+} channels by glucose metabolism in mouse pancreatic B-cells. *Nature* 342:550–553, 1989
13. Ashcroft FM, Rorsman P: Electrophysiology of the pancreatic β-cell. *Prog Biophys Mol Biol* 54:87–143, 1989
14. Plant TD: Properties of calcium-dependent inactivation of calcium channels in cultured mouse pancreatic β-cells. *J Physiol* 404:731–747, 1988
15. Hiriart M, Matteson DR: Na channels and two types of Ca^{2+} channels in rat pancreatic B-cells identified with the reverse Hemolytic Plaque Assay. *J Gen Physiol* 91:617–639, 1988
16. Misler S, Barnett DW, Gillis KD, Pressel DM: Electrophysiology of stimulus-secretion coupling in human β-cells. *Diabetes* 41:1221–1228, 1992
17. Barnett DW, Pressel DM, Misler S: Voltage-dependent Na^+ and Ca^{2+} currents in human pancreatic islet β-cells: evidence for roles in the generation of action potentials and insulin secretion. *Pflügers Arch* 431:272–282, 1995
18. Ashcroft FM, Kelly RP, Smith PA: Two types of Ca channel in rat pancreatic β-cells. *Pflügers Arch* 415:504–506, 1990
19. Fox AP, Nowycky MC, Tsien RW: Kinetic and pharmacological properties distinguishing three types of calcium currents in chick sensory neurones. *J Physiol* 394:149–172, 1987
20. Narahashi T, Tsunoo A, Yoshii M: Characterization of two types of calcium channels in mouse neuroblastoma cells. *J Physiol* 383:231–249, 1987
21. Hagiwara N, Irisawa H, Kameyama M: Contribution of two types of calcium currents to the pacemaker potentials of rabbit sino-atrial node cells. *J Physiol* 395:233–253, 1988
22. Tang C-M, Presser F, Morad M: Amiloride selectively blocks the low threshold (T) calcium channel. *Science* 240:213–215, 1988
23. Tytgat J, Vereecke J, Carmeliet E: Mechanism of cardiac T-type Ca^{2+} channel blockade by amiloride. *J Pharmacol Exp Ther* 254:546–551, 1990
24. Mogul DJ, Fox AP: Evidence for multiple types of Ca^{2+} channels in acutely isolated hippocampal CA3 neurones of the guinea-pig. *J Physiol* 433:259–281, 1991
25. Barrett PQ, Isales CM, Bollag WB, McCarthy RT: Ca^{2+} channels and aldosterone secretion: modulation by K^+ and atrial natriuretic peptide. *Am J Physiol* 30:F706–F719, 1991
26. Gu X, Spitzer NC: Low-threshold Ca^{2+} current and its role in spontaneous elevations of intracellular Ca^{2+} in developing *Xenopus* neurons. *J Neurosci* 13:4936–4948, 1993
27. Sen L, Smith TW: T-type Ca^{2+} channels are abnormal in genetically determined cardiomyopathic hamster hearts. *Circ Res* 75:149–155, 1994
28. Nuss HB, Houser SR: T-type Ca^{2+} current is expressed in hypertrophied adult feline left ventricular myocytes. *Circ Res* 73:777–782, 1993
29. Schmitt R, Clozel Z-P, Iberg N, Bühler FR: Mibefradil prevents neointima formation after vascular injury in rats, possible role of the blockade of the T-type voltage-operated calcium channel. *Arterioscler Thromb Vasc Biol* 15:1161–1165, 1995
30. Coulter DA, Huguenard JR, Prince DA: Specific petit mal anticonvulsants reduce calcium currents in thalamic neurons. *Neurosci Lett* 98:74–78, 1989
31. Buisson B, Bottari SP, de Gasparo M, Gallo-Payet N, Payet MD: The angiotensin AT_2 receptor modulates T-type calcium current in non-differentiated NG108-15 cells. *FEBS Lett* 209:161–164, 1992
32. Furukawa T, Ito H, Nitta J, Tsujino M, Adachi S, Hiroe M, Marumo F, Sawanobori T, Hiraoka M: Endothelin-1 enhances calcium entry through T-type calcium channels in cultured neonatal rat ventricular myocytes. *Circ Res* 71:1242–1253, 1992
33. Wang Z, Estacion M, Mordan LJ: Ca^{2+} influx via T-type channels modulates PDGF-induced replication of mouse fibroblasts. *Am J Physiol* 865:C1239–C1246, 1993
34. Trump BF, Berezesky IK: Calcium-mediated cell injury and cell death. *FASEB J* 9:219–228, 1995
35. Smith PA, Ashcroft FM, Fewtrell CMS: Permeation and gating properties of the L-type calcium channel in mouse pancreatic β-cells. *J Gen Physiol* 101:767–797, 1993
36. Hopkins WF, Satin LS, Cook DL: Inactivation kinetics and pharmacology distinguish two calcium currents in mouse pancreatic B-cells. *J Membr Biol* 119:229–239, 1991